Synthesis and Characterization of First-Row Transition Metal Tellurolates. X-ray Crystal Structures of $Mn[TeSi(SiMe_3)_3]_2(dmpe)$, $Fe[TeSi(SiMe_3)_3]_2(dmpe)_2$, $Fe[TeSi(SiMe_3)_3](Cl)(dmpe)_2$, and $Co[TeSi(SiMe_3)_3](PMe_3)_3$

David E. Gindelberger and John Arnold*

Department of Chemistry, University of California, Berkeley, California 94720

Received June 29, 1993®

The syntheses of several first-row transition metal tellurolate derivatives incorporating the sterically encumbered ligand -$TeSi(SiMe_3)_3$ are described. Metathesis reactions of $MCl_2(dmpe)_2$ (M = Cr, Mn, Fe) or $CoBr_2(PMe_3)_3$ with $[(THF)_2LiTeSi(SiMe_3)_3]_2$ yield $M[TeSi(SiMe_3)_3]_2(dmpe)_2$ and $Co[TeSi(SiMe_3)_3](PMe_3)_3$, respectively. Tellurolysis of the transition metal amides $M[N(SiMe_3)_2]_2$ with $HTeSi(SiMe_3)_3$ in the presence of Lewis bases yields $M[TeSi(SiMe_3)_3]_2L_2$ (M = Mn, L = 4-*tert*-butylpyridine or $^1/_2$ dmpe (dmpe = 1,2-bis(dimethylphosphino)-ethane); M = Fe, L = dmpe). The compounds have been characterized by a combination of NMR spectroscopy, magnetic measurements, and elemental analyses. In addition, four derivatives have been structurally characterized by X-ray crystallography. $Mn[TeSi(SiMe_3)_3]_2(dmpe)_2$ crystallizes in the space group $P2_12_12_1$ with a = 13.104(3) Å, b = 25.523(6) Å, c = 28.504(4) Å, V = 9533(5) Å^3, d_{calc} = 1.33 g cm^{-1}, Z = 8, R = 3.90%, and R_w = 3.96%. Crystal data for $Fe[TeSi(SiMe_3)_3]_2(dmpe)_2$: space group $P\bar{1}$ with a = 9.556(2) Å, b = 9.814(2) Å, c = 32.990(5) Å, V = 2672.4(8) Å^3, d_{calc} = 1.37 g cm^{-1}, Z = 2, R = 6.13%, and R_W = 7.09%. $Fe[TeSi(SiMe_3)_3](Cl)(dmpe)_2$ crystallizes in the space group $P2_1/c$ with a = 9.317(2) Å, b = 11.898(2) Å, c = 32.836(7) Å, V = 3637(1) Å^3, d_{calc} = 1.40 g cm^{-1}, Z = 4, R = 3.31%, and R_w = 3.52%. The crystal structure of $Co[TeSi(SiMe_3)_3](PMe_3)_3$ was also determined; it crystallizes in the space group $P2_1/c$ with a = 17.651(5) Å, b = 12.435(3) Å, c = 17.704(4) Å, V = 3418(1) Å^3, d_{calc} = 1.29 g cm^{-1}, Z = 4, R = 5.92%, and R_w = 7.67%.

Introduction

In recent efforts to develop the chemistry of metal tellurolates and selenolates,[1,2] we have focused our attention on derivatives involving -$ESi(SiMe_3)_3$ ligands (E = Se, Te).[3-12] These ligands are remarkably versatile as evidenced by the wide range of complexes they form with transition metal and main group elements. In general, the resulting complexes are easy to isolate and purify since they are stable at ambient temperature and dissolve in inert hydrocarbon solvents from which are readily crystallized. Here we describe our work on first-row transition metal derivatives of Cr, Mn, Fe, and Co incorporating the -$TeSi(SiMe_3)_3$ ligand. In contrast to the more well-studied alkoxide and thiolate derivatives of these metals,[13,14] the list of known tellurolate derivatives of these metals is quite short, and most of these are binuclear or multinuclear species stabilized by carbonyl or Cp ligands. These include, for example, manganese complexes such as $[(Cp(CO)_2Mn)_2TePh]^x$ ($x = \pm 1$),[15] $[Mn(TePh)_4]^{2-}$,[16] $[(CpMn(CO)_2)_3(\mu_3\text{-}TeMe)]$,[17] and $Mn(CO)_3(PEt_3)_2(TeCH_2Ph)$,[18] a number of iron tellurolates such as $[Fe_4Te_4(TePh)_4]^{3-}$.[19] $CpFe(CO)_2TeR$, $[CpFe(CO)TeR]_2$,[20,21] and related iron carbonyl species,[22-24] and the cobalt derivative $[Cp_2Nb(\mu\text{-}TePh)_2Co(CO)_2]$.[25]

* Abstract published in *Advance ACS Abstracts*, November 1, 1993.

(1) Gysling, H. J. *Coord. Chem. Rev.* **1982**, *42*, 133.
(2) Gysling, H. J. In *The Chemistry of Organic Selenium and Tellurium Compounds*; Patai, S., Rappoport, Z., Ed.; Wiley: New York, 1986; Vol. 1, p 679.
(3) Gindelberger, D. E.; Arnold, J. *J. Am. Chem. Soc.* **1992**, *114*, 6242.
(4) Bonasia, P. J.; Gindelberger, D. E.; Dabbousi, B. O.; Arnold, J. *J. Am. Chem. Soc.* **1992**, *114*, 5209.
(5) Bonasia, P. J.; Christou, V.; Arnold, J. *J. Am. Chem. Soc.* **1993**, *115*, 6777.
(6) Cary, D. R.; Arnold, J. *J. Am. Chem. Soc.* **1993**, *114*, 2520.
(7) Christou, V.; Arnold, J. *J. Am. Chem. Soc.* **1992**, *114*, 6240.
(8) Seligson, A. L.; Bonasia, P. J.; Arnold, J.; Yu, K. M.; Walker, J. M.; Bourret, E. D. *Mater. Res. Soc. Symp. Proc.* **1992**, *282*, 665.
(9) Bonasia, P. J.; Arnold, J. *Inorg. Chem.* **1992**, *31*, 2508.
(10) Bonasia, P. J.; Arnold, J. *J. Organomet. Chem.* **1993**, *449*, 147.
(11) Arnold, J.; Walker, J. M.; Yu, K. M.; Bonasia, P. J.; Seligson, A. L.; Bourret, E. D. *J. Cryst. Growth* **1992**, *124*, 674.
(12) Seligson, A. L.; Arnold, J. *J. Am. Chem. Soc.* **1993**, *115*, 8214.
(13) For reviews of alkoxides, see: Bradley, D. C.; Mehrotra, R. C.; Gaur, D. P. *Metal Alkoxides*; Academic: New York, 1978. Mehrotra, R. C. *Adv. Inorg. Chem. Radiochem.* **1983**, *26*, 269. Rothwell, I. P.; Chisholm, M. H. In *Comprehensive Coordination Chemistry*; Wilkinson, G., Gillard, R. D., McCleverty, J. A., Eds.; Pergamon: New York, 1987; Vol. 2; p 335.
(14) For recent examples, see the following and references therein: Yu, S. B.; Papaefthymiou, G. C.; Holm, R. H. *Inorg. Chem.* **1991**, *30*, 3476. Treichel, P. M.; Rublein, E. K. *J. Organomet. Chem.* **1992**, *424*, 71. Santos, R. A.; Gruff, E. S.; Koch, S. A.; Harbison, G. S. *J. Am. Chem. Soc.* **1991**, *113*, 469. Silver, A.; Koch, S. A.; Millar, M. *Inorg. Chim. Acta* **1993**, *205*, 9. Krebs, B.; Henkel, G. *Angew. Chem., Int. Ed. Engl.* **1991**, *30*, 769. Bouwman, E.; Bolcar, M. A.; Libby, E.; Huffman, J. C.; Folting, K.; Christou, G. *Inorg. Chem.* **1992**, *31*, 5185. Labahn, D.; Brooker, S.; Sheldrick, G. M.; Roesky, H. W. Z. *Anorg. Allg. Chem.* **1992**, *610*, 163. Dance, I. G. *Polyhedron* **1986**, *5*, 1037. Blower, P. G.; Dilworth, J. R. *Coord. Chem. Rev.* **1987**, *76*, 121. Block, E.; Ofori-Okai, G.; Kang, H.; Wu, J.; Zubieta, J. *Inorg. Chim. Acta* **1991**, *190*, 5. Nicholson, J. R.; Christou, G.; Wang, R. J.; Huffman, J. C.; Chang, H. R.; Hendrickson, D. N. *Polyhedron* **1991**, *10*, 2255. Springs, J.; Janzen, C. P.; Darensbourg, M. Y.; Calabrese, J. C.; Krusic, P. J.; Verpeaux, J. N.; Amatore, C. *J. Am. Chem. Soc.* **1990**, *112*, 5789. Ruhlandt-Senge, K.; Power, P. P. *J. Chem. Soc., Dalton Trans.* **1993**, 649. Edema, J. J. H.; Gambarotta, S.; Smeets, W. J. J.; Spek, A. L. *Inorg. Chem.* **1991**, *30*, 1380. Bartlett, R. A.; Ellison, J. J.; Power, P. P.; Shoner, S. C. *Inorg. Chem.* **1991**, *30*, 2888. Shoner, S. C.; Power, P. P. *Inorg. Chem.* **1992**, *31*, 1001. Garg, G.; Dubey, R. K.; Singh, A.; Mehrotra, R. C. *Polyhedron* **1991**, *10*, 1733. Mandal, S. K.; Ho, D. M.; Orchin, M. *Organometallics* **1993**, *12*, 1714. Gupta, R.; Singh, A.; Mehrotra, R. C. *Indian J. Chem., Sect. A* **1993**, *32*, 310.
(15) Huttner, G.; Schuler, S.; Zsolnai, L.; Gottlieb, M.; Braunwarth, H.; Minelli, M. *J. Organomet. Chem.* **1986**, *299*, C4.
(16) Tremel, W.; Krebs, B.; Greiwe, K.; Simon, W.; Stephan, H.-O.; Henkel, G. *Z. Naturforsch.* **1992**, *47B*, 1580.
(17) Herrmann, W. A.; Hecht, C.; Herdtweck, E. *J. Organomet. Chem.* **1987**, *331*, 309.
(18) McGregor, K.; Deacon, G. B.; Dickson, R. S.; Fallon, G. D.; Rowe, R. S.; West, B. O. *J. Chem. Soc., Chem. Commun.* **1990**, 1293.
(19) Simon, W.; Wilk, A.; Bernt, K.; Henkel, G. *Angew. Chem., Int. Ed. Engl.* **1987**, *26*, 1009.
(20) Cobbledick, R. E.; Dance, N. S.; Einstein, F. W. B.; Jones, C. H. W.; Jones, T. *Inorg. Chem.* **1981**, *20*, 4356.
(21) Schermer, E. D.; Baddley, W. H. *J. Organomet. Chem.* **1971**, *27*, 83.
(22) Kostiner, E.; Reddy, M. L. N.; Urch, D. S.; Massey, A. G. *J. Organomet. Chem.* **1968**, *15*, 383.
(23) Liaw, W.-F.; Chiang, M.-H.; Liu, C.-J.; Harn, P.-J.; Liu, L.-K. *Inorg. Chem.* **1993**, *32*, 1536.
(24) Bachman, R. E.; Whitmire, K. H. *Organometallics* **1993**, *12*, 1988.

0020-1669/93/1332-5813$04.00/0

Table I. Physical Data for New Compounds

compound	yield/%	color	mp/°C	μ_{eff}/μ_B
$Cr[TeSi(SiMe_3)_3]_2(dmpe)_2$	74	orange	179–181	2.7 ± 0.1
$Mn[TeSi(SiMe_3)_3]_2(dmpe)$	80	orange	>450	5.9 ± 0.1
$Mn[TeSi(SiMe_3)_3]_2(4\text{-}^tBuNC_5H_4)_2$	41	lt yellow	177–179	5.9 ± 0.1
$Fe[TeSi(SiMe_3)_3]_2(dmpe)_2$	79	dk green	174–176	diamag
$Fe[TeSi(SiMe_3)_3](Cl)(dmpe)_2$	88	orange	166–168	diamag
$Co[TeSi(SiMe_3)_3](PMe_3)_3$	64	dk orange	154–157	3.8 ± 0.1
$Co(CO)_2[TeSi(SiMe_3)_3](PMe_3)_2$	76	red	94–97	diamag

Results and Discussion

Our initial attempts focused on the preparation of the simplest tellurolate derivatives, the binary or homoleptic tellurolates $M(TeR)_n$. However, treatment of divalent first-row metal halides of Cr, Mn, Fe, Co, and Ni with 2 equiv of $(THF)_2LiTeSi(SiMe_3)_3$ was unsuccessful, leading only to formation of substantial quantities of the ditelluride $[TeSi(SiMe_3)_3]_2$ along with insoluble, pyrophoric solids. These reactions are presumably analogous to redox processes using CuCl that are used to synthesize ditellurides on preparative scales.[4]

Tellurolysis of metal amides, such as $M[N(SiMe_3)_2]_2$ (M = Mn, Fe) with 2 equiv of $HTeSi(SiMe)_3$ in hexane yielded extremely soluble, oily materials from which we could not isolate pure compounds. In these cases, however, addition of Lewis donors such as pyridines or phosphines rapidly formed tractable derivatives that we were able to isolate by crystallization. For example, the manganese derivative crystallizes as the four-coordinate monodmpe adduct (eq 1). Isolation of the yellow bis(pyridine) analogue

$$Mn[N(SiMe_3)_2]_2(THF) + 2HTeSi(SiMe)_3 + \text{dmpe (excess)} \rightarrow Mn[TeSi(SiMe_3)_3]_2(dmpe) + 2HN(SiMe_3)_2 \quad (1)$$

$Mn[TeSi(SiMe_3)_3]_2(4\text{-}^tBuC_5H_4N)_2$ in a similar reaction serves to further confirm this metal's preference for four coordination in divalent complexes with bulky tellurolates. Physical data for these compounds are collected in Table I. Both Mn derivatives are paramagnetic, with ^1H NMR spectra exhibiting extremely broad $-TeSi(SiMe_3)_3$ signals (fwhm ca. 300 Hz) at δ 4.7 ppm and 2.5 ppm for the dmpe and *tert*-butylpyridine complexes, respectively.

Addition of dmpe to the dark, oily solid resulting from reaction between 2 equiv of $HTeSi(SiMe_3)_3$ and $Fe[N(SiMe_3)_2]_2$ gave dark green toluene-soluble crystals of $Fe[TeSi(SiMe_3)_3]_2(dmpe)_2$ in good yield after crystallization from Et_2O (eq 2). It appears

$$Fe[N(SiMe_3)_2]_2 + 2HTeSi(SiMe)_3 + 2dmpe \rightarrow Fe[TeSi(SiMe_3)_3]_2(dmpe)_2 + 2HN(SiMe_3)_2 \quad (2)$$

that the homoleptic species $M[TeSi(SiMe_3)_3]_2$ are indeed formed under these conditions, but we are unable to isolate them in pure form as a result of their extreme solubility.

Metathesis reactions met with more success when they were carried out either in the presence of donor ligands, or using the known adducts $MX_2(dmpe)_2$.[26] Yields and product purities obtained from these reactions were similar to those obtained by tellurolysis. For Fe(II), tellurolate ligands may be added sequentially as shown below:

$$FeCl_2(dmpe)_2 \xrightarrow{+TeR^-} Fe[TeSi(SiMe_3)_3]Cl(dmpe)_2 \xrightarrow{+TeR^-} Fe[TeSi(SiMe_3)_3]_2(dmpe)_2 \quad (3)$$

$$R = Si(SiMe_3)_3$$

Both $Fe[TeSi(SiMe_3)_3]_2(dmpe)_2$ and $Fe[TeSi(SiMe_3)_3]Cl(dmpe)_2$ are diamagnetic, showing similar ^1H and ^{31}P shifts for the dmpe and $-TeSi(SiMe_3)_3$ ligands. By virtue of its lower symmetry, the mono tellurolate shows inequivalent dmpe methyl and methylene protons in its ^1H NMR spectrum and inequivalent methyls in the ^{13}C NMR spectrum. The latter complex was also prepared by the redistribution reaction shown in eq 4. Further evidence

$$Fe[TeSi(SiMe_3)_3]_2(dmpe)_2 + FeCl_2(dmpe)_2 \rightarrow 2Fe[TeSi(SiMe_3)_3]Cl(dmpe)_2 \quad (4)$$

suggesting lability of tellurolate ligands in $Fe[TeSi(SiMe_3)_3]_2(dmpe)_2$ was obtained from conductivity measurements in acetonitrile which gave molar conductivity values in the range expected for a 1:1 electrolyte.[27] Under these conditions, acetonitrile displaces a single tellurolate ligand to form the salt $\{[Fe[TeSi(SiMe_3)_3](dmpe)_2(MeCN)\}[TeSi(SiMe_3)_3]$, which was subsequently isolated in good yield by recrystallization of the ditellurolate from acetonitrile. The MeCN appears to be weakly bound since the CN stretching frequency (2244 cm^{-1}) is shifted only slightly from that of free MeCN (2254 cm^{-1}).[28,29] In noncoordinating solvents such as nitromethane and toluene the complex is nonconducting. This reactivity is reminiscent of the behavior of $FeCl_2(depe)_2$ (depe = $Et_2PCH_2CH_2PEt_2$) which, under similar conditions, undergoes displacement of one chloride to form $[FeCl(MeCN)(depe)_2]^+$ (ν_{CN} at 2242 cm^{-1}).[29-31] The *mono*tellurolate also behaves as a 1:1 electrolyte in acetonitrile, but again in common with $FeCl_2(depe)_2$, the acetonitrile ligand is labile and the starting material is recovered upon removal of solvent under vacuum.

Metathesis chemistry was also successful in the synthesis of chromium tellurolates. For example, high yields of the orange, paramagnetic Cr(II) derivative were obtained as shown in eq 5.

$$CrCl_2(dmpe)_2 + [(THF)_2LiTeSi(SiMe_3)_3]_2 \rightarrow Cr[TeSi(SiMe_3)_3]_2(dmpe)_2 + 2LiCl \quad (5)$$

In the case of Co(II) shown below (eq 6), we again observed reduction of the metal center, although in this case the reduced product is formed in good yield. The dark orange monotellurolate complex is quite stable, and both it and the ditelluride byproduct were isolated by fractional crystallization from hexane at −40 °C.

$$CoBr_2(PMe_3)_3 + 2(THF)_2LiTeSi(SiMe_3)_3 \rightarrow Co[TeSi(SiMe_3)_3](PMe_3)_3 + {}^1/_2[TeSi(SiMe_3)_3]_2 \quad (6)$$

Room temperature solid state magnetic susceptibility data (Table I) show that $Cr[TeSi(SiMe_3)_3]_2(dmpe)_2$ and $Co[TeSi(SiMe_3)_3](PMe_3)_3$ are low-spin systems (d^4 and d^8 respectively) with two unpaired electrons on each metal. The two d^5 tetrahedral manganese complexes are high-spin, with solid-state suscepti-

(25) Sato, M.; Yoshida, T. *J. Organomet. Chem.* **1975**, *94*, 403.
(26) Girolami, G. S.; Wilkinson, G.; Galas, A. M. R.; Thornton-Pett, M.; Hursthouse, M. B. *J. Chem. Soc., Dalton Trans.* **1985**, 1339.
(27) Geary, W. J. *Coord. Chem. Rev.* **1971**, *7*, 81.
(28) Nakamoto, K. *Infrared and Raman Spectra of Inorganic and Coordination Compounds*, 3rd ed.; John Wiley and Sons: New York, 1978.
(29) Storhoff, B. N.; Lewis, H. C. J. *Coord. Chem. Rev.* **1977**, *23*, 1.
(30) Bellerby, J. M.; Mays, M. J.; Sears, P. L. *J. Chem. Soc., Dalton Trans.* **1976**, 1232.
(31) Bellerby, J. M.; Mays, M. J. *J. Chem. Soc., Dalton Trans.* **1975**, 1281.

bilities close to the spin-only value for five unpaired electrons. This paramagnetism results in broad, shifted resonances in the ^1H NMR spectra of these compounds, with signals due to the tellurolate ligand in the range of 2–4 ppm downfield from those in related diamagnetic species. Although the dmpe protons were not detected, the PMe_3 protons in $Co[TeSi(SiMe_3)_3](PMe_3)_3$ gave rise to a broad, low-field signal at 70 ppm. In neither the Cr(II) nor Mn(II) dmpe complex were we able to detect ^{31}P signals.

In common with related 16-electron Co(I) tetrahedral species,[32-34] $Co[TeSi(SiMe_3)_3](PMe_3)_3$ reacts readily with excess CO to form a diamagnetic five-coordinate complex (eq 7).

$$Co[TeSi(SiMe_3)_3](PMe_3)_3 + CO\ (1\ atm) \rightarrow Co(CO)_2[TeSi(SiMe_3)_3](PMe_3)_2 + PMe_3 \quad (7)$$

Although there was no noticeable color change during the reaction, red crystals of the dicarbonyl were isolated from acetonitrile in 76% yield. The ^1H NMR spectrum of the product displays a virtual triplet for the PMe_3 ligands and a sharp singlet for the $SiMe_3$ groups. A sharp singlet was also seen in the $^{31}P\{^1H\}$ spectrum. In contrast, the ^{125}Te resonance is broad at room temperature and only broadens further on cooling, rendering it of little use in the structure assignment. Since the carbonyl resonance could not be detected in the ^{13}C NMR spectrum (even at low temperature), the compound labeled with ^{13}CO (99% ^{13}C) was prepared. At room temperature, this showed a broad triplet at 203 ppm in the ^{13}C NMR spectrum along with a slightly broadened ^{31}P signal. At −70 °C both resonances sharpened and split into triplets with $J_{P-C} = 28$ Hz. Taken together, these NMR data imply stereochemical nonrigidity of the type commonly observed in pentacoordinate species, in which the square pyramidal and trigonal bypyramidal structures interconvert rapidly on the NMR time scale.[35] Two strong CO absorptions observed in the IR lend further support to this idea, with ν_{sym} and ν_{asym} at 1963 and 1903 cm^{-1} (1916 and 1859 cm^{-1} in the ^{13}C labeled complex). These data are similar to those reported in related species such as $CoI(CO)_2(PEt_3)_2$ which displays ν_{CO} at 1975 and 1905 cm^{-1}.[36]

We found no evidence for reactions of $Co[TeSi(SiMe_3)_3](PMe_3)_3$ with ethylene or PMe_3 at room temperature in benzene, despite the fact that reactions with related Co(I) species are known.[32-34,37,38]

In common with nearly all complexes of the $-TeSi(SiMe_3)_3$ ligand, the complexes described here are sensitive to air and moisture, but are otherwise stable at 20 °C under nitrogen. The oxidation and hydrolysis products are invariably ditelluride and tellurol respectively. The manganese derivative appears to be the most sensitive, decomposing within seconds on exposure to air. All of the compounds are soluble in nonpolar hydrocarbon solvents to varying degrees, with the dmpe and pyridine adducts being moderately soluble and the cobalt phosphine derivative showing intense solubility. In contrast to group 12 derivatives of the $-TeSi(SiMe_3)_3$ ligand,[9] none of the compounds showed molecular ions in their 70-eV electron impact mass spectra, evidently due to decomposition upon heating. Attempts to sublime the compounds (100–200 °C, 10^{-3} Torr) were also unsuccessful, again due to thermal decomposition.

X-ray Crystallographic Studies. The molecular structure of $Mn[TeSi(SiMe_3)_3]_2(dmpe)$ is shown as an ORTEP view in Figure 1, with crystallographic data in Table II and pertinent bond lengths and angles given in Table III. There are two independent molecules in the unit cell that are identical chiral pairs. The compound is isostructural with $Cd[TeSi(SiMe_3)_3]_2(dmpe)$,[9] displaying remarkably similar features such as an acute P–M–P angle (80.39(10)° compared to 78.50(8)° in the latter) and a Te1–M–Te2 angle of 142.45(6)° that is identical to that in the Cd species, within experimental error (142.35(3)°). The Mn–P bond lengths (2.603 Å average) are in the range found in other tetrahedral manganese phosphine compounds (2.528–2.674 Å).[39-41] At 2.690(2) Å, the Mn–Te bond length is slightly shorter than other experimentally determined Mn–Te distances in four-coordinate $[Mn(TePh)_4]^-$ (2.722–2.760 Å) or six-coordinate $Mn(TeCH_2Ph)(CO)_3(PEt_3)_2$ (2.705(1) Å).

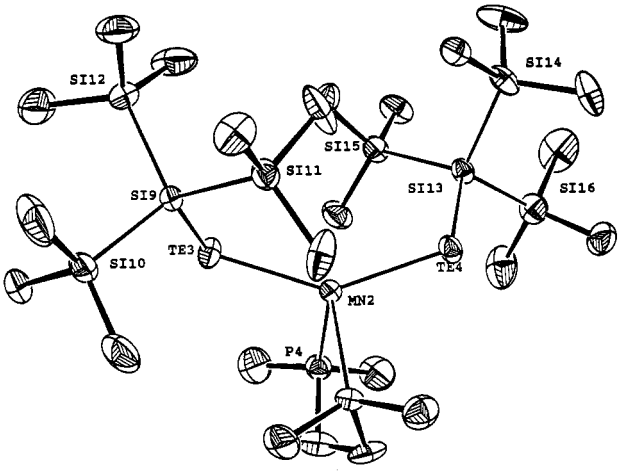

Figure 1. ORTEP view of the molecular structure of $Mn[TeSi(SiMe_3)_3]_2(dmpe)$.

The structure of $Fe[TeSi(SiMe_3)_3]_2(dmpe)_2$ is shown in Figure 2, with bond lengths and angles in Table IV. The iron is coordinated by two *trans*-tellurolates and two dmpe ligands in an octahedral fashion. The dmpe ligands in this compound are severely disordered. The molecule has strict inversion symmetry, which results in the three trans interactions having angles of 180°. The average P–Fe–P angle is 90.0° which is larger than found in other $ML_2(dmpe)_2$ structures (77.8–85.8°).[26,42] The Fe–P bond lengths (2.246 Å average) are only slightly longer than those found in $(dmpe)_2FeCl_2$ (2.235 Å average).[42] The Fe–Te bond length (2.723(1) Å) may be compared to that found in other structurally characterized iron tellurolates such as $[Fe_4Te_4(TePh)_4]^{3-}$ (Fe–TePh range from 2.589 to 2.606 Å[19]); it is considerably longer than any other known Fe–Te bond lengths (2.536–2.646 Å),[19,20,23,24] but is shorter than the estimated bond length based on ionic radii (2.82 Å).[43]

Figure 3 shows the structure of the related species $Fe[TeSi(SiMe_3)_3](Cl)(dmpe)_2$. The Fe–Te bond is shorter than that found in the bis-tellurolate (2.682 Å), but is still longer than those found in other iron tellurolates described above. The P–Fe–P angles, and Cl–Fe–P angles (Table V) are similar to those found in $FeCl_2(dmpe)_2$.[42] The Fe–Cl bond (2.379 Å) is longer than found in related iron bis(dialkylphosphino)ethane complexes (2.344–2.352 Å),[42,44] and the average Fe–P distance (2.234 Å) is identical to that found in the dichloride.

A view of the solid-state structure of $Co[TeSi(SiMe_3)_3](PMe_3)_3$ is given in Figure 4. The angles around the pseudotetrahedral

(32) Klein, H. F.; Karsch, H. H. *Chem. Ber.* **1975**, *108*, 944.
(33) Klein, H. F.; Karsch, H. H. *Inorg. Chem.* **1975**, *14*, 473.
(34) Klein, H. F.; Ellrich, K.; Neugebauer, D.; Orama, O.; Krüger, K. *Z. Naturforsch.* **1983**, *38B*, 303.
(35) Muetterties, E. L. *Acc. Chem. Res.* **1970**, *3*, 266.
(36) Bordignon, E.; Croatto, U.; Mazzi, U.; Orio, A. A. *Inorg. Chem.* **1974**, *13*, 935.
(37) Klein, H. F.; Hammer, R.; Gross, J.; Schubert, U. *Angew. Chem., Int. Ed. Engl.* **1980**, *19*, 809.
(38) Capelle, B.; Beauchamp, A. L.; Dartiguenave, M.; Dartiguenave, Y.; Klein, H. F. *J. Am. Chem. Soc.* **1982**, *104*, 3891.
(39) Howard, C. G.; Girolami, G. S.; Wilkinson, G.; Thornton-Pett, M.; Hursthouse, M. B. *J. Chem. Soc., Dalton Trans.* **1983**, 2631.
(40) Hebendanz, N.; Köhler, F. H.; Müller, G. *Inorg. Chem.* **1984**, *23*, 3043.
(41) Howard, C. G.; Girolami, G. S.; Wilkinson, G.; Thornton-Pett, M.; Hursthouse, M. B. *J. Am. Chem. Soc.* **1984**, *106*, 2033.
(42) Di Vaira, M.; Midollini, S.; Sacconi, L. *Inorg. Chem.* **1981**, *20*, 3430.
(43) Shannon, R. D.; Prewitt, C. T. *Acta Crystallogr.* **1969**, *B25*, 925. Shannon, R. D. *Acta Crystallogr.* **1976**, *A32*, 751.
(44) Baker, M. V.; Field, L. D.; Hambley, T. W. *Inorg. Chem.* **1988**, *27*, 2872,.

Table II. Summary of X-ray Diffraction Data

	$Mn[TeSi(SiMe_3)_3]_2(dmpe)$	$Fe[TeSi(SiMe_3)_3]_2(dmpe)_2$	$Fe[TeSi(SiMe_3)_3](Cl)(dmpe)_2$	$Co[TeSi(SiMe_3)_3](PMe_3)_3$
formula	$Te_2MnP_2Si_8C_{24}H_{76}$	$Te_2FeP_4Si_8C_{30}H_{86}$	$TeFeP_4Si_8ClC_{21}H_{59}$	$TeCoP_3Si_4C_{18}H_{54}$
mol wt	961.03	1105.96	1146.98	662.17
T/°C	−100	−91	−105	−92
space group	$P2_12_12_1$	$P\bar{1}$	$P2_1/c$	$P2_1/c$
a/Å	13.104(3)	9.556(2)	9.317(2)	17.651(5)
b/Å	25.523(6)	9.814(2)	11.898(2)	12.435(3)
c/Å	28.504(4)	32.990(5)	32.836(7)	17.704(4)
α/deg	90.0	83.82(1)	90.0	90.0
β/deg	90.0	84.77(1)	92.13(2)	118.40(2)
γ/deg	90.0	60.46(1)	90.0	90.0
vol/Å^3	9533.2(6)	2674.2(8)	3637(1)	3418(1)
Z	8	2	4	4
d_{calcd}/g cm^{-3}	1.33	1.37	1.40	1.29
cryst size/mm	0.45 × 0.45 × 0.21	0.25 × 0.20 × 0.10	0.28 × 0.18 × 0.13	0.40 × 0.40 × 0.20
scan mode	ω	ω	θ–2θ	θ–2θ
2θ range/deg	3–50	3–45	3–45	3–45
collcn range	$+h,+k,+l$	$+h,\pm k,\pm l$	$+h,+k,\pm l$	$+h,+k,\pm l$
absn coeff/cm^{-1}	17.5	16.7	15.9	16.3
no. of unique reflns	9137	6975	6147	4860
no. of reflns with $F^2 > 3\sigma(F^2)$	6710	4712	3688	3511
final R, R_w	0.0390, 0.0396	0.0613, 0.0709	0.0331, 0.0352	0.0592, 0.0767

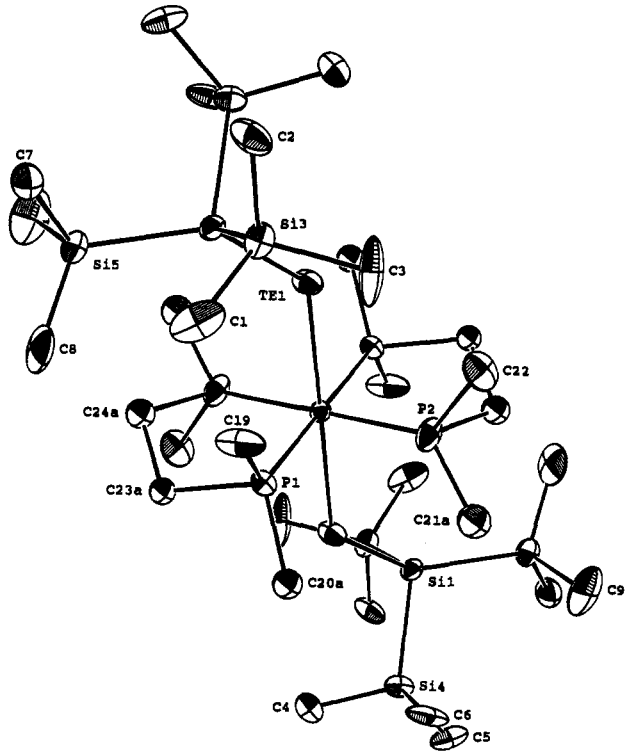

Figure 2. ORTEP view of the molecular structure of $Fe[TeSi(SiMe_3)_3]_2(dmpe)_2$.

Table III. Selected Metrical Parameters for $Mn[TeSi(SiMe_3)_3]_2(dmpe)$

	Bond Distances (Å)		
Mn1–Te1	2.690(2)	Mn1–Te2	2.669(2)
Mn1–P1	2.600(3)	Mn1–P2	2.605(3)
Te1–Si1	2.519(3)	Te2–Si5	2.502(3)
	Bond Angles (deg)		
Te1–Mn1–Te2	142.45(6)	P1–Mn1–P2	80.39(10)
Te1–Mn1–P1	96.79(8)	Te1–Mn1–P2	110.08(8)
Te2–Mn1–P1	114.70(8)	Te2–Mn1–P2	95.52(8)
Mn1–Te1–Si1	109.49(7)	Mn1–Te2–Si5	116.47(8)

cobalt range from 94.59(7) to 127.27(8)° (Table VI). The Co–P distances are similar to those found in $(PMe_3)_3CoI$ (2.232(2), 2.237(1) Å).[45] Although we are unaware of other cobalt(I) tellurolates that may be used for comparison, our observed Co–Te bond length (2.543 Å) is similar to Co–Te interactions in cobalt *tellurido* species (2.451–2.584 Å).[46,47]

Parameters associated with the $-TeSi(SiMe_3)_3$ moiety in all four structures (Tables II–V) are similar to values found for other structures containing this ligand.[3,4,6,7,9] Also in common

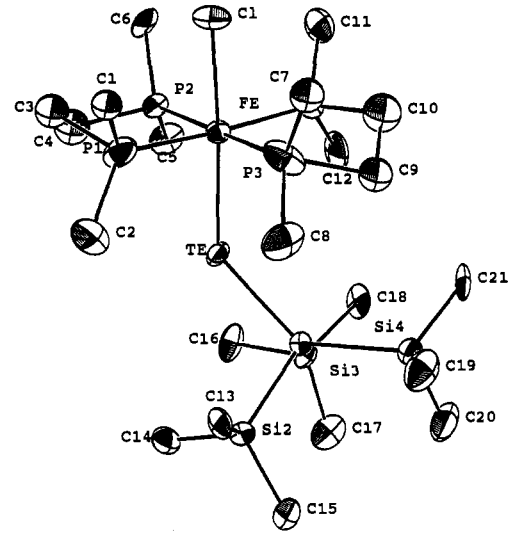

Figure 3. ORTEP view of the molecular structure of $Fe[TeSi(SiMe_3)_3](dmpe)_2Cl$.

Table IV. Selected Metrical Parameters for $Fe[TeSi(SiMe_3)_3]_2(dmpe)_2$

	Bond Distances (Å)		
Fe1–Te1	2.721(1)	Fe1–P1	2.250(4)
Te1–Si1	2.537(4)	Fe1–P2	2.241(4)
	Bond Angles (deg)		
Fe1–Te1–Si1	133.23(10)	Te1–Fe1–P2	90.46(11)
Te1–Fe1–P1	95.31(10)		
	Bond Distances (Å)		
Fe2–Te2	2.724(1)	Fe2–P3	2.245(4)
Te2–Si2	2.542(4)	Fe2–P4	2.247(4)
	Bond Angles (deg)		
Fe2–Te2–Si2	133.49(10)	Te2–Fe2–P4	89.82(11)
Te2–Fe2–P3	95.73(10)		

(45) Bandy, J. A.; Green, J. C.; Kirchner, O. N. *Acta Crystallogr.* **1985**, *C41*, 1179.

(46) Rheingold, A. L. *Acta Crystallogr.* **1987**, *C43*, 585.

(47) Klein, H. F.; Gass, M.; Koch, U.; Eisenmann, B.; Schäfer, H. *Z. Naturforsch.* **1988**, *43B*, 830.

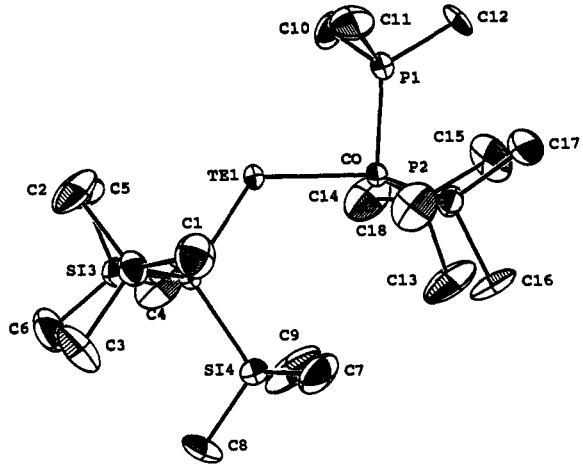

Figure 4. ORTEP view of the molecular structure of Co[TeSi(SiMe$_3$)$_3$](PMe$_3$)$_3$.

Table V. Selected Metrical Parameters for Fe[TeSi(SiMe$_3$)$_3$](dmpe)$_2$Cl

	Bond Distances (Å)		
Fe–Te	2.682(1)	Fe–P3	2.217(3)
Fe–Cl	2.379(3)	Fe–P4	2.225(4)
Fe–P1	2.236(4)	Te–Si1	2.546(3)
Fe–P2	2.259(3)		
	Bond Angles (deg)		
P1–Fe–P2	85.63(12)	P1–Fe–P4	175.63(13)
P1–Fe–P3	93.52(13)	P2–Fe–P3	178.23(13)
P2–Fe–P4	94.55(12)	Fe–Te–Si1	133.80(8)
P3–Fe–P4	86.19(13)		

Table VI. Selected Metrical Parameters for Co[TeSi(SiMe$_3$)$_3$](PMe$_3$)$_3$

	Bond Distances (Å)		
Te1–Co	2.543(1)	Co–P2	2.227(3)
Te1–Si1	2.494(2)	Co–P3	2.227(3)
Co–P1	2.248(3)	Co–Te–Si1	123.34(7)
	Bond Angles (deg)		
Te1–Co–P1	94.59(7)	P1–Co–P2	103.21(11)
Te1–Co–P2	118.71(8)	P1–Co–P3	102.25(10)
Te1–Co–P3	127.27(8)	P2–Co–P3	105.47(10)

with previously determined structures, the M–Te–Si angle varies considerably among the four compounds, from 116.47° in the manganese case to 123.34° for the cobalt species and to 133.80° in the iron monotellurolate. There were no unusually close intermolecular contacts present in any of the four structures.

Experimental Section

Unless noted otherwise all operations were carried out under a dry nitrogen atmosphere using a combination of glovebox and Schlenk techniques. Tetrahydrofuran, diethyl ether, toluene, and hexanes (all from Fisher) were predried over 4-Å molecular sieves and distilled from sodium/benzophenone under N_2. Acetonitrile (Fisher) was predried as above, stirred over calcium hydride for 1 week, and then distilled under N_2. All NMR solvents were dried similarly, but were distilled by vacuum transfer. Dmpe was prepared by the literature method.[48] Melting points were determined in sealed capillaries under nitrogen and are uncorrected. IR samples were prepared as Nujol mulls between KBr plates or taken in solution between CaF_2 windows as noted. Chemical shifts (δ) for ^{1}H NMR spectra are relative to residual protium in the deuterated solvents listed (e.g. C_6D_6, δ 7.15 ppm). Chemical shifts for ^{125}Te NMR spectra are relative to external Te(OH)$_6$ in D_2O (1.74 M) at δ 712 ppm, and were performed at ambient temperatures in 5-mm tubes at 94.5726 MHz. Magnetic moments were determined using a Johnson-Mathey MSB-1 balance. Conductivities were measured in acetonitrile using a Fisher Digital Conductivity Meter. Elemental analyses were performed at the microanalytical laboratory of the College of Chemistry, University of California, Berkeley, CA.

Cr[TeSi(SiMe$_3$)$_3$]$_2$(dmpe)$_2$. To 0.26 g of (dmpe)$_2$CrCl$_2$[26] suspended in 20 mL of hexanes was added 0.62 g (0.59 mmol) of [(THF)$_2$LiTeSi(SiMe$_3$)$_3$]$_2$[4] dissolved in hexane (20 mL). The mixture immediately turned deep orange. After the mixture was stirred for 30 min, the solvent was removed under reduced pressure, the residue was extracted with Et$_2$O (40 mL). The ether solution was concentrated to 20 mL and cooled to −40 °C. Two crops of dark orange crystals were collected (0.48 g, 74%). Mp: 179–181 °C (dec). ^{1}H NMR (400 MHz, C_6D_6): δ 3.55 (br s, $w_{1/2}$ = 148 Hz). IR: 1416 m, 1405 m, 1290 m, 1276 m, 1254 m, 1242 s, 1233 s, 1116 w, 1073 w, 986 w, 940 s, 926 s, 910 m, 885 m, 860 s, 834 s, 786 m, 727 m, 699 m, 683 s, 635 m, 621 s cm^{-1}. Anal. Calcd for $C_{30}H_{86}Te_2FeP_4Si$: C, 32.7; H, 7.86. Found: C, 33.1; H, 7.84.

Mn[TeSi(SiMe$_3$)$_3$]$_2$(dmpe). Method A. To 0.30 g (0.67 mmol) of (THF)Mn[N(SiMe$_3$)$_2$]$_2$[49] and 0.50 g (1.3 mmol) of HTeSi(SiMe$_3$)$_3$[4] in hexanes (20 mL) was added 0.22 mL (1.3 mmol) of dmpe. Immediately the solution turned orange and small needles begin to precipitate. The mixture was stirred for 20 min, and the solvent was removed under reduced pressure. The residue was extracted with Et$_2$O (50 mL), and the filtrate was concentrated and cooled. In two crops, 0.50 g (79%) of dark orange crystals were collected.

Method B. To 0.60 g (9.5 mmol) of (dmpe)$_2$MnI$_2$[26] suspended in 25 mL of toluene was added 1.0 g (0.95 mmol) of [(THF)$_2$LiTeSi(SiMe$_3$)$_3$]$_2$ in 25 mL of toluene. The mixture gradually became orange as the (dmpe)$_2$MnI$_2$ dissolved. After 1 h the solvent was removed under reduced pressure and the residue was extracted with Et$_2$O (50 mL). The filtrate was concentrated and cooled to −20 °C. Dark orange crystals were collected by filtration (0.85 g, 80%). At 153 °C the material turns dark red, but does not melt below 450 °C. ^{1}H NMR (300 MHz, C_6D_6): δ 4.51 ($w_{1/2}$ = 480 Hz). IR: 1416 s, 1302 s, 1284 s, 1245 s, 1236 s, 1138 m, 1087 m, 996 w, 948 s, 928 s, 890 m, 840 s, 738 s, 706 s, 685 s, 645 m, 622 s cm^{-1}. Anal. Calcd for $C_{24}H_{70}Te_2MnP_2Si_8$: C, 30.2; H, 7.38. Found: C, 30.3; H, 6.91.

Mn[TeSi(SiMe$_3$)$_3$]$_2$(4-Bu^t-pyridine)$_2$. To a solution of 0.30 g (0.67 mmol) of (THF)Mn[N(SiMe$_3$)$_2$]$_2$ in 25 mL of hexane was added 0.50 g (1.3 mmol) of HTeSi(SiMe$_3$)$_3$ in 20 mL of hexane. The solution changed from pale pink to dark orange immediately. A 0.19-mL (1.3-mmol) portion of 4-*tert*-butylpyridine was added to the mixture, and the deep orange solution changed to a light green color. The mixture was stirred for 3 min before becoming cloudy and finally precipitating a pale-yellow feathery solid. The solvents were removed under reduced pressure, and the crude product was collected (0.58 g, 81%). Recrystallization from diethyl ether yielded 0.29 g (41%) of pale-yellow feathery crystals. Mp: 177–179 °C. ^{1}H NMR (300 MHz, C_6D_6): δ 2.8 (br s, $w_{1/2}$ = 1000 Hz), 2.41 (br s, $w_{1/2}$ = 393 Hz). IR: 1616 m, 1504 w, 1420 m, 1307 w, 1279 w, 1244 s, 1068 w, 1019 m, 864 s, 836 s, 745 w, 723 m, 688 m, 625 m, 569 m cm^{-1}. Anal. Calcd for $C_{36}H_{80}Te_2MnSi_8N_2$: C, 40.2; H, 7.49; N, 2.60. Found: C, 39.8; H, 7.36; N, 2.66.

Fe[TeSi(SiMe$_3$)$_3$]$_2$(dmpe)$_2$. Method A. To 0.25 g (0.66 mmol) of Fe[N(SiMe$_3$)$_2$]$_2$[50] and dmpe (0.22 mL, 1.3 mmol) in hexanes (25 mL) was added a solution of 0.50 g (1.3 mmol) of HTeSi(SiMe$_3$)$_3$ in hexanes (25 mL). The mixture turned dark orange, and a crystalline solid began to precipitate. The solution was stirred for 1 h, and the solvent was removed under reduced pressure. The residue was extracted with Et$_2$O (50 mL), and the filtrate was concentrated and cooled. Dark green crystals of the product were collected in two crops (0.52 g, 71%).

Method B. Toluene (40 mL) was added to 1.2 g (2.7 mmol) of (dmpe)$_2$FeCl$_2$[26] and 2.9 g (2.7 mmol) of [(THF)$_2$LiTeSi(SiMe$_3$)$_3$]$_2$. The resulting deep orange solution was stirred for 6 h and the solvent was removed under reduced pressure. The residue was extracted with toluene (100 mL). The mixture was filtered through a Schlenk frit, and the material remaining on the frit was washed with more toluene (25 + 10 mL). The combined filtrates were concentrated and cooled to −40 °C. The product was obtained as dark green crystals (2.4 g, 79%). Mp: 174–176 °C. ^{1}H NMR (400 MHz, C_6D_6): δ 1.99 (m, 4 H), 1.76 (s, 12 H), 0.36 (s, 27 H). ^{13}C{^{1}H} NMR (100 MHz, C_6D_6): δ 32.1 (m, *C*H$_2$), 23.6 (t, *C*H$_3$), 2.8 (s, Si(*C*H$_3$)$_3$). ^{31}P{^{1}H} NMR (162 MHz, C_6D_6): δ 49.1 (s, J_{P-Te} = 79 Hz). ^{125}Te{^{1}H} NMR: δ −1189 (q, J_{Te-P} = 80 Hz). IR: 1416 w, 1405 w, 1293 w, 1276 w, 1253 w, 1243 m, 1232 m, 938 m, 926 m, 911 w, 886 w, 859 sh, 834 s, 722 m, 697 w, 682 m, 622 m, cm^{-1}.

(48) Burt, R. J.; Chatt, J.; Hussain, W.; Leigh, G. J. *J. Organomet. Chem.* **1979**, *182*, 203.

(49) Bürger, H.; Wannagat, U. *Monatsh. Chem.* **1964**, *95*, 1099.

(50) Andersen, R. A.; Faegri Jr., K.; Green, J. C.; Haaland, A.; Lappert, M. F.; Leung, W.; Rypdal, K. *Inorg. Chem.* **1988**, *27*, 1782.

Λ_m(4.5 × 10^{-4} M) = 182 Ω^{-1} cm^2 mol^{-1}. Anal. Calcd for $C_{30}H_{86}Te_2FeP_4Si_8$: C, 33.0; H, 7.83. Found: C, 33.1; H, 8.06.

Fe[TeSi(SiMe$_3$)$_3$]$_2$(dmpe)$_2$(MeCN). Fe[TeSi(SiMe$_3$)$_3$]$_2$(dmpe)$_2$ (1.5 g, 1.4 mmol) was stirred in MeCN (100 mL) for 2 h over which time the solid gradually dissolved to give an orange solution. The solution was filtered, the volume was reduced to 20 mL and cooled to −40 °C overnight. Orange crystals were obtained in 67% yield (0.70 g). Mp: 151–153 °C. IR: 2244 m, 1415 m, 1302 m, 1283 m, 1230 s, 940 s, 915 m, 839 m, 830 s, 736 m, 705 m, 683 m, 648 m, 623 m, 462 m cm^{-1}. ^{1}H NMR (400 MHz, CD_3CN): δ 2.42 (m, 4 H), 2.22 (m, 4 H), 2.11 (s, 3 H), 2.04 (br s, 12 H), 1.92 (br s, 12 H), 0.30 (s, 27 H), 0.28 (s, 27 H). ^{31}P{^{1}H} NMR (121 MHz, CD_3CN)): δ 64.9 (s, J_{P-C} = 76 Hz). Anal. Calcd for $C_{31}H_{89}Te_2FeP_4Si_8N$: C, 34.5; H, 7.82; N, 1.22. Found: C, 34.9; H, 7.68; N, 1.38.

Fe[TeSi(SiMe$_3$)$_3$](Cl)(dmpe)$_2$. Method A. To 0.08 g (0.18 mmol) of $FeCl_2$(dmpe)$_2$ and 0.20 g (0.18 mmol) of Fe[TeSi(SiMe$_3$)$_3$]$_2$(dmpe)$_2$ was added THF (30 mL). The reaction mixture was stirred for 1 h, and the solvent was removed under reduced pressure. The residue was extracted with hexanes (100 mL) and filtered. The volume was reduced to 20 mL and cooled to −40 °C. Two crops of dark orange needles were collected (0.23 g, 82%).

Method B. THF (30 mL) was added to a mixture of 1.1 g (2.5 mmol) of $FeCl_2$(dmpe)$_2$ and 1.3 g (1.2 mmol) of [(THF)$_2$LiTeSi(SiMe$_3$)$_3$]$_2$. The reaction mixture was stirred for 3 h, and the orange residue was extracted with hexanes (3 × 100 mL). The extracts were combined, the volume was reduced to 100 mL and cooled to −40 °C. This yielded 1.7 g (88%) of dark orange crystals. Mp: 166–168 °C. ^{1}H NMR (400 MHz, C_6D_6): δ 2.04 (m, 4 H), 1.87 (m, 4 H), 1.71 (s, 12 H), 1.32 (s, 12 H), 0.34 (s, 27 H). ^{13}C{^{1}H} NMR (100 MHz, C_6D_6): δ 3.11 (m, *C*H$_2$), 21.1 (t, *C*H$_3$), 13.9 (t, *C*H$_3$), 2.67 (s, Si(*C*H$_3$)$_3$). ^{31}P{^{1}H} NMR (162 MHz, C_6D_6): δ 56.4 (s, J_{Te-P} = 76 Hz). ^{125}Te{^{1}H} NMR: δ −1350 (q, J_{Te-P} = 78 Hz). IR: 1415 m, 1281 m, 1237 s, 1076 w, 934 s, 888 m, 832 s, 724 m, 699 m, 644 w, 624 m cm^{-1}. Λ_m (1.3 × 10^{-3} M) = 132 Ω^{-1} cm^2 mol^{-1}. Anal. Calcd for $C_{21}H_{59}ClTeFeP_4Si_4$: C, 32.9; H, 7.75. Found: C, 33.4; H, 7.79.

Co[TeSi(SiMe$_3$)$_3$](PMe$_3$)$_3$. To a solution of 1.6 g (3.3 mmol) of $CoBr_2(PMe_3)_3$·0.5(toluene)[51] dissolved in toluene (20 mL) was added 3.4 g (3.2 mmol) of [(THF)$_2$LiTeSi(SiMe$_3$)$_3$]$_2$ in toluene (20 mL). After the mixture was stirred for 2 h, the solvent was removed under reduced pressure and the dark yellow residue was extracted with hexanes (50 mL). The extract was concentrated and cooled to −40 °C to give 1.7 g of product in two crops. Recrystallization from hexanes yielded 1.4 g (64%) of dark orange-yellow crystals. Mp: 154–157 °C. ^{1}H NMR (400 MHz, C_6D_6): δ 70.5 (br s, 27 H), 1.60 (br s, 27 H). IR: 1421 m, 1415 m, 1295 m, 1277 m, 1252 w, 1234 s, 956 m, 932 s, 860 sh, 832 s, 742 w, 713 s, 685 s, 656 s, 621 s cm^{-1}. Anal. Calcd for $C_{18}H_{54}TeCoP_3Si_4$: C, 32.6; H, 8.22. Found: C, 32.6; H, 8.25.

Co(CO)$_2$[TeSi(SiMe$_3$)$_3$](PMe$_3$)$_2$. Co[TeSi(SiMe$_3$)$_3$](PMe$_3$)$_3$ (0.20 g, 0.30 mmol) dissolved in hexanes (50 mL) was stirred under an atmosphere of CO for 12 h. The solvent was removed under reduced pressure, the residue was extracted with acetonitrile (20 mL), then filtered. The volume was reduced to 5 mL and cooled to −40 °C. Dark red needles of the product (0.15 g) were obtained in 76% yield. Mp: 94–97 °C. ^{1}H NMR (400 MHz, C_6D_6): δ 1.42 ("t", 18 H, J_{H-P} = 4 Hz), 0.48 (s, 27 H). ^{13}C{^{1}H} NMR (75 MHz, C_6D_6): δ 21.5 ("t", J_{C-P} = 18 Hz, P(*C*H$_3$)$_3$), 2.8 (s, Si(*C*H$_3$)$_3$). ^{31}P{^{1}H} NMR (121 MHz, C_6D_6): δ 15.4 (br s). ^{125}Te{^{1}H} NMR: δ −1417 (br s, $\Delta\nu_{1/2}$ = 110 Hz). IR (C_6D_6): 2948 m, 1916 s, 1859 s, 1831 m, 1283 m, 1241 m cm^{-1}. Anal. Calcd for $C_{17}H_{45}O_2TeCoP_2Si_4$: C, 31.8; H, 7.06. Found: C, 31.6; H, 6.70.

X-ray Crystallography. The crystal structures of all but the cobalt derivative were solved by Patterson methods; the former was solved by direct methods.[52] The data was then refined via standard least-squares and Fourier techniques. Table II contains the details of the crystal data collection parameters. The determination of the manganese structure was carried out by Dr. F. J. Hollander. The structure of Fe[TeSi(SiMe$_3$)$_3$](Cl)(dmpe)$_2$ was determined by students in the College of Chemistry's crystallography course under the supervision of Dr. Hollander.

Fe[TeSi(SiMe$_3$)$_3$]$_2$(dmpe)$_2$. Transparent dark green plates were obtained by crystallization from a saturated Et_2O/THF solution at −20 °C. An appropriate crystal (0.25 × 0.20 × 0.10 mm) was mounted on a glass fiber using Paratone N hydrocarbon oil. The crystal was transferred to the diffractometer, centered in the beam and cooled to −91 °C.

(51) Bressan, M.; Rigo, P. *Inorg. Chem.* **1975**, *14*, 38.
(52) Sheldrick, G. M. *Crystallographic Computing 3*; Oxford University: Oxford, England, 1985; p 175.

Table VII. Positional Parameters for Mn[TeSi(SiMe$_3$)$_3$]$_2$(dmpe)[a]

atom	*x*	*y*	*z*	*B*/Å^2
Te1	0.63447(1)	0.70275(1)	0.95080(1)	2.55(1)
Te2	0.60330(1)	0.85432(1)	0.83650(1)	3.11(1)
Mn1	0.6592(1)	0.79731(1)	0.91068(1)	2.27(3)
P1	0.6804(2)	0.8502(1)	0.98803(9)	2.98(6)
P2	0.8526(2)	0.8200(1)	0.90497(9)	3.01(6)
Si1	0.6496(2)	0.63240(9)	0.88921(9)	2.17(5)
Si2	0.6567(2)	0.55499(9)	0.93359(9)	2.40(6)
Si3	0.7970(2)	0.6394(1)	0.8435(1)	3.16(6)
Si4	0.5070(2)	0.6351(1)	0.8406(1)	2.63(6)
Si5	0.4226(2)	0.8859(1)	0.8354(1)	2.30(5)
Si6	0.3633(3)	0.8736(1)	0.7583(1)	3.51(7)
Si7	0.4264(3)	0.9763(1)	0.8514(1)	3.29(7)
Si8	0.3151(2)	0.8419(1)	0.8881(1)	2.91(6)
Cl	0.761(1)	0.5597(4)	0.9771(4)	4.7(3)
C2	0.535(1)	0.5466(4)	0.9670(4)	5.1(3)
C3	0.6769(9)	0.4963(3)	0.8959(3)	3.3(2)
C4	0.807(1)	0.7060(4)	0.8162(4)	4.5(3)
C5	0.7918(9)	0.5896(4)	0.7960(4)	4.0(3)
C6	0.9122(9)	0.6281(5)	0.8808(4)	4.8(3)
C7	0.3887(9)	0.6456(4)	0.8760(4)	3.8(2)
C8	0.493(1)	0.5723(4)	0.8070(4)	4.8(3)
C9	0.5218(9)	0.6899(5)	0.7979(4)	4.3(3)
C10	0.386(1)	0.8053(5)	0.7373(4)	5.1(3)
C11	0.433(1)	0.9182(5)	0.7179(4)	5.9(4)
C12	0.224(1)	0.8872(6)	0.7538(5)	7.3(4)
C13	0.3032(9)	1.0081(5)	0.8365(6)	6.4(4)
C14	0.527(1)	1.0083(5)	0.8166(5)	5.9(4)
C15	0.454(1)	0.9882(5)	0.9149(5)	7.5(5)
C16	0.3814(9)	0.8265(5)	0.9440(4)	5.2(3)
C17	0.1997(9)	0.8833(5)	0.9016(4)	4.4(3)
C18	0.265(1)	0.7803(4)	0.8609(5)	6.4(4)
C19	0.651(1)	0.8211(5)	1.0431(4)	5.4(3)
C20	0.628(2)	0.9157(5)	0.9944(6)	9.8(5)
C21	0.819(1)	0.8599(5)	0.9924(4)	5.3(3)
C22	0.867(1)	0.8732(5)	0.9479(4)	5.3(3)
C23	0.909(1)	0.8483(5)	0.8520(4)	5.4(3)
C24	0.9448(9)	0.7718(5)	0.9240(5)	5.1(3)
Te3	0.87966(1)	0.65256(1)	0.67002(1)	2.57(1)
Te4	0.85798(1)	0.80462(1)	0.55564(1)	2.52(1)
Mn2	0.8180(1)	0.71349(1)	0.59936(1)	2.03(3)
P3	0.7814(2)	0.6594(1)	0.52429(9)	2.33(5)
P4	0.6221(2)	0.7000(1)	0.60906(9)	2.62(5)
Si9	1.0614(2)	0.6230(1)	0.66213(9)	2.11(5)
Si10	1.0606(2)	0.5318(1)	0.6518(1)	2.87(6)
Si11	1.1472(2)	0.6666(1)	0.60128(9)	2.62(6)
Si12	1.1455(2)	0.6432(1)	0.73261(9)	2.88(6)
Si13	0.8460(2)	0.87981(9)	0.61277(9)	2.19(5)
Si14	1.0026(2)	0.9237(1)	0.6091(1)	2.88(6)
Si15	0.8142(2)	0.8549(1)	0.69065(9)	2.86(6)
Si16	0.7190(3)	0.9361(1)	0.5843(1)	3.44(7)
C25	0.9855(9)	0.4984(4)	0.6993(4)	3.9(3)
C26	1.194(1)	0.5071(4)	0.6537(5)	5.9(4)
C27	1.002(1)	0.5142(4)	0.5949(4)	5.2(3)
C28	1.0736(9)	0.6640(5)	0.5449(4)	4.3(3)
C29	1.161(1)	0.7366(4)	0.6186(4)	5.6(3)
C30	1.2782(8)	0.6389(5)	0.5918(4)	3.9(3)
C31	1.122(1)	0.5933(5)	0.7785(4)	5.3(3)
C32	1.2853(8)	0.6448(5)	0.7234(4)	4.3(3)
C33	1.104(1)	0.7085(5)	0.7556(4)	5.2(3)
C34	1.1095(8)	0.8767(4)	0.6169(4)	3.2(2)
C35	1.0161(9)	0.9561(4)	0.5504(4)	4.5(3)
C36	1.014(1)	0.9742(4)	0.6570(5)	5.5(3)
C37	0.7032(9)	0.8091(4)	0.6954(4)	4.1(3)
C38	0.929(1)	0.8225(5)	0.7151(4)	5.2(3)
C39	0.784(1)	0.9148(4)	0.7257(3)	4.0(3)
C40	0.589(1)	0.9079(5)	0.5937(5)	5.9(3)
C41	0.733(1)	0.9471(4)	0.5202(4)	4.6(3)
C42	0.731(1)	1.0022(4)	0.6139(5)	7.0(4)
C43	0.8312(9)	0.6792(4)	0.4681(4)	3.8(3)
C44	0.802(1)	0.5889(4)	0.5233(4)	4.2(3)
C45	0.6429(9)	0.6658(4)	0.5169(3)	3.8(2)
C46	0.5897(9)	0.6527(4)	0.5626(4)	4.4(3)
C47	0.5366(9)	0.7538(5)	0.5968(5)	5.0(3)
C48	0.571(1)	0.6715(5)	0.6615(4)	5.3(3)

[a] The thermal parameter given for anisotropically refined atoms is the isotropic equivalent thermal parameter defined as: (4/3)[$a^2\beta$(1,1) + $b^2\beta$(2,2) + $c^2\beta$(3,3) + ab(cos γ)β(1,2) + ac(cos β)β(1,3) + bc(cos α)β(2,3)], where *a*, *b*, and *c* are real cell parameters and $\beta(i,j)$ are anisotropic βs.

Table VIII. Positional Parameters for $Fe[TeSi(SiMe_3)_3]_2(dmpe)_2$

atom	x	y	z	B/Å²
Te1	−0.0918(1)	0.1951(1)	0.06146(1)	2.05(2)
Te2	0.3797(1)	0.2257(1)	0.43749(1)	2.45(2)
Fe1	0.000	0.000	0.000	1.23(6)
Fe2	0.500	0.000	0.500	1.31(6)
P1	0.2406(4)	0.8251(4)	0.0250(1)	1.72(9)
P2	0.1151(4)	0.1302(4)	0.9648(1)	2.6(1)
P3	0.4378(4)	0.8332(4)	0.4752(1)	1.85(9)
P4	0.2577(5)	0.1112(5)	0.5331(1)	3.0(1)
Si1	0.0177(4)	0.8471(4)	0.8646(1)	1.56(9)
Si2	0.3379(4)	0.2199(4)	0.3628(1)	1.52(9)
Si3	0.1947(4)	0.2066(4)	0.1419(1)	2.1(1)
Si4	0.2603(4)	0.6313(4)	0.8422(1)	2.2(1)
Si5	0.0242(4)	0.9386(4)	0.1828(1)	2.1(1)
Si6	0.0712(4)	0.2725(5)	0.3541(1)	2.5(1)
Si7	0.3490(5)	0.4523(4)	0.3410(1)	2.5(1)
Si8	0.4886(5)	0.9712(5)	0.6819(1)	2.5(1)
C1	0.392(2)	0.024(2)	0.1549(5)	3.5(4)
C2	0.144(2)	0.340(2)	0.1828(5)	2.9(4)
C3	0.229(2)	0.306(2)	0.0938(5)	4.7(4)
C4	0.282(2)	0.446(2)	0.8702(5)	3.4(5)
C5	0.277(2)	0.604(2)	0.7857(5)	3.4(4)
C6	0.435(2)	0.657(2)	0.8533(5)	3.5(5)
C7	0.066(2)	0.987(2)	0.2325(5)	2.8(4)
C8	0.203(2)	0.747(2)	0.1712(5)	4.6(5)
C9	0.155(2)	0.094(2)	0.8078(6)	4.9(5)
C10	0.022(2)	0.578(2)	0.6896(5)	4.8(5)
C11	0.059(2)	0.645(2)	0.5979(5)	5.5(6)
C12	0.063(2)	0.089(2)	0.3444(6)	4.8(5)
C13	0.464(3)	0.174(2)	0.6705(6)	7.6(7)
C14	0.419(2)	0.108(2)	0.2664(5)	5.2(6)
C15	0.277(2)	−0.003(2)	0.6859(6)	6.3(6)
C16	0.185(2)	0.623(2)	0.3687(6)	4.3(5)
C17	0.451(2)	0.573(2)	0.6482(6)	5.0(5)
C18	0.319(2)	0.515(2)	0.2845(6)	5.0(5)
C19	0.311(2)	0.874(2)	0.0678(4)	3.4(4)
C20b	0.305(3)	0.611(3)	0.0320(9)	2.5(6)*
C20a	0.435(3)	0.711(3)	0.9952(8)	2.1(6)*
C21a	0.286(3)	0.063(3)	0.9300(9)	2.8(7)*
C21b	0.139(4)	0.137(4)	0.911(1)	4.8(9)*
C22	0.111(2)	0.304(1)	0.9814(5)	3.3(4)
C23b	0.400(3)	0.824(3)	0.9872(9)	0.24(6)*
C23a	0.219(3)	0.660(3)	0.0558(8)	1.7(5)*
C24a	0.045(3)	0.739(3)	0.0783(9)	2.2(6)*
C24b	0.356(3)	0.998(3)	0.9733(9)	2.9(7)*
C25a	0.282(3)	0.926(3)	0.4341(8)	1.5(5)*
C25b	0.353(3)	0.876(3)	0.4265(9)	2.3(6)*
C26a	0.410(3)	0.376(3)	0.5292(9)	2.9(7)*
C26b	0.357(3)	0.715(3)	0.504(1)	3.2(7)*
C27b	0.227(3)	0.103(3)	0.5861(9)	2.6(6)*
C27a	0.162(4)	0.026(4)	0.568(1)	4.1(8)*
C28	0.082(2)	0.290(2)	0.5154(6)	3.9(5)
C29a	0.284(3)	0.798(3)	0.511(1)	3.4(7)*
C29b	0.387(3)	0.312(3)	0.5528(9)	2.4(6)*
C30b	0.292(3)	0.227(3)	0.5767(9)	2.9(7)*
C30a	0.153(4)	0.979(4)	0.521(1)	4.4(8)*

Automatic peak search and indexing procedures yielded a triclinic reduced primitive cell. Analysis of normalized structure factors indicated that the structure was centrosymmetric. The choice of the centric space group $P\bar{1}$ was confirmed by the successful solution and refinement of the structure. Hydrogen atoms on the tellurolate ligands were assigned idealized locations and were included in structure factor calculations, but were not refined. The final residuals for 400 variables refined against 4712 data for which $F^2 > 3\sigma(F^2)$ were $R = 0.0613$, $R_w = 0.0709$, and GOF = 2.67. There are two half-molecules in the asymmetric unit each containing one dmpe, one tellurolate ligand, and one-half iron atom. The carbon atoms in the dmpe molecules were disordered and were refined isotropically with an occupancy of 0.50 for the methylenes and 0.50 for five of the eight methyl groups. The ordered methyl groups (C19, C22, C28) were refined anisotropically.

$Mn[TeSi(SiMe_3)_3]_2(dmpe)$. Large clear orange platelike crystals of the compound were obtained by slowly cooling a saturated ether solution to −40 °C. The crystal (0.45 × 0.45 × 0.21 mm) was mounted as above and cooled to −100 °C. Automatic peak search and indexing procedures yielded an orthorhombic reduced primitive cell. Inspection of the systematic absences indicated the space group $P2_12_12_1$. Hydrogen atoms were assigned idealized locations and were included in structure factor calculations, but were not refined. The final residuals for 667 variables refined against 6710 data for which $F^2 > 3\sigma(F^2)$ were $R = 0.0390$, $R_w = 0.0396$, and GOF = 1.30.

Table IX. Positional Parameters for $Fe[TeSi(SiMe_3)_3](dmpe)_2Cl$

atom	x	y	z	B/Å²
Te	0.17377(7)	0.44036(1)	0.09582(1)	2.55(2)
Fe	0.1403(1)	0.2196(1)	0.08199(1)	1.76(4)
Cl	0.1063(3)	0.0264(2)	0.06560(9)	3.03(8)
P1	0.2627(3)	0.2363(3)	0.0250(1)	3.48(9)
P2	−0.0553(3)	0.2630(2)	0.0424(1)	2.18(7)
P3	0.3333(3)	0.1723(2)	0.1196(1)	3.90(9)
P4	0.0168(3)	0.1890(2)	0.1376(1)	2.88(9)
Si1	0.2598(3)	0.5555(2)	0.1573(1)	1.71(8)
Si2	0.4417(3)	0.6619(2)	0.1274(1)	2.06(8)
Si3	0.0655(3)	0.6764(2)	0.1700(1)	2.14(8)
Si4	0.3502(3)	0.4944(2)	0.2217(1)	2.46(8)
C1	0.387(1)	0.107(1)	0.0132(5)	2.5(3)*
C2	0.393(1)	0.3439(9)	0.0159(4)	4.7(4)
C3	0.147(1)	0.226(1)	−0.0192(5)	3.4(4)*
C4	0.002(1)	0.3070(9)	−0.0070(4)	4.2(3)*
C5	−0.1817(9)	0.3742(8)	0.0543(3)	3.2(3)
C6	−0.178(1)	0.1503(8)	0.0272(3)	3.2(3)
C7	0.405(1)	0.032(1)	0.1226(5)	3.1(4)*
C8	0.490(1)	0.2566(9)	0.1243(4)	4.5(3)
C9	0.286(1)	0.196(1)	0.1768(5)	3.5(4)*
C10	0.140(1)	0.1367(9)	0.1783(4)	4.7(3)*
C11	−0.126(1)	0.0850(9)	0.1371(4)	4.5(3)
C12	−0.073(1)	0.3029(9)	0.1643(4)	4.3(3)
C13	0.5847(9)	0.5678(8)	0.1085(3)	2.7(3)
C14	0.365(1)	0.7409(8)	0.0833(3)	3.0(3)
C15	0.5303(9)	0.7626(8)	0.1624(3)	2.8(3)
C16	−0.028(1)	0.7192(9)	0.1216(3)	3.4(3)
C17	0.125(1)	0.8093(8)	0.1951(4)	3.9(3)
C18	−0.067(1)	0.6058(9)	0.2027(3)	3.4(3)
C19	0.536(1)	0.4362(9)	0.2203(4)	4.3(3)
C20	0.363(1)	0.6214(9)	0.2543(4)	4.3(3)
C21	0.231(1)	0.398(1)	0.2500(4)	4.4(3)
C1′	0.295(3)	0.145(3)	−0.016(1)	3.5(8)*
C3′	0.127(3)	0.360(3)	−0.010(1)	2.8(8)*
C7′	0.453(3)	0.054(3)	0.086(1)	2.2(7)*
C9′	0.294(3)	0.061(3)	0.151(1)	3.7(8)*

Table X. Positional Parameters for $Co[TeSi(SiMe_3)_3](PMe_3)_3$

atom	x	y	z	B/Å²
Te1	0.81968(1)	0.09622(1)	0.05320(1)	3.94(2)
Co	0.82078(7)	−0.10733(9)	0.06953(1)	2.16(3)
P1	0.9379(2)	−0.01092(2)	0.1998(1)	2.86(6)
P2	0.8602(2)	−0.2091(2)	−0.0096(1)	3.35(6)
P3	0.7279(1)	−0.2071(2)	0.0911(1)	2.73(5)
Si1	0.6981(1)	0.1969(2)	−0.0635(1)	2.16(5)
Si2	0.6358(2)	0.2952(2)	0.0050(2)	3.32(6)
Si3	0.7642(2)	0.3147(2)	−0.1171(2)	3.17(6)
Si4	0.5990(2)	0.0847(2)	−0.1700(2)	3.24(6)
C1	0.6007(6)	0.2051(9)	0.0655(6)	4.9(3)
C2	0.7194(7)	0.391(1)	0.0839(6)	5.9(3)
C3	0.5378(7)	0.125(1)	0.4250(7)	5.8(3)
C4	0.8069(6)	0.237(1)	−0.1817(6)	6.4(3)
C5	0.8607(7)	0.379(1)	−0.0248(7)	5.7(3)
C6	0.6891(7)	0.4230(9)	−0.1847(7)	5.9(3)
C7	0.5523(8)	−0.009(1)	−0.1204(7)	7.4(4)
C8	0.5089(8)	0.165(1)	−0.2569(7)	7.1(4)
C9	0.6555(8)	0.007(1)	−0.2192(8)	9.3(4)
C10	1.0327(6)	−0.0334(9)	0.2050(7)	4.7(3)
C11	0.9207(7)	−0.040(1)	0.2834(6)	5.0(3)
C12	0.9932(7)	−0.2335(8)	0.2576(6)	5.2(3)
C13	0.7713(8)	−0.264(1)	−0.1121(7)	7.6(4)
C14	0.0801(8)	0.132(1)	0.0547(7)	7.2(4)
C15	0.0757(9)	0.168(1)	0.4597(8)	8.0(4)
C16	0.6423(6)	−0.2799(9)	−0.0017(6)	4.7(3)
C17	0.7685(6)	−0.3143(9)	0.1728(6)	4.6(3)
C18	0.6631(6)	−0.128(1)	0.1276(6)	5.3(3)

$Fe[TeSi(SiMe_3)_3](Cl)(dmpe)_2$. Large orange plates were grown from concentrated hexanes by slowly cooling to −40 °C. The crystal (0.18 × 0.28 × 0.13 mm) was mounted as described above and cooled to −105 °C. Automatic peak search and indexing procedures yielded an orthorhombic reduced primitive cell. Inspection of the systematic absences

indicated the space group $P2_1/c$. Hydrogen atoms were assigned idealized locations and were included in structure factor calculations, but were not refined. As in $Fe[TeSi(SiMe_3)_3]_2(dmpe)_2$, the carbons in the dmpe molecules were partially disordered. The disordered methyls (C1, C7) and methylenes (C3, C9) were placed in two different positions, with the occupancy set to 70% and 30% and refined isotropically. The final residuals for 275 variables refined against 3688 data for which $F^2 > 3\sigma(F^2)$ were $R = 0.0331$, $R_w = 0.0353$, and GOF = 1.07.

$Co[TeSi(SiMe_3)_3](PMe_3)_3$. Very large opaque crystals were grown from a concentrated hexane solution. An appropriate crystal (0.40 × 0.40 × 0.20) was cleaved from a larger crystal mounted as above, and cooled to −92 °C. Automatic peak search and indexing procedures yielded a monoclinic reduced primitive cell. Inspection of the systematic absences indicated the space group $P2_1/c$. Hydrogen atoms were assigned idealized locations and were included in structure factor calculations, but were not refined. The final residuals for 244 variables refined against 3506 data for which $F^2 > 3\sigma(F^2)$ were $R = 0.0592$, $R_w = 0.0767$, and GOF = 2.53.

Acknowledgment. We are grateful to the National Science Foundation for financial support, and we thank William Fuller, Stefan Ruprecht and Todd Friedman for determining one of the crystal structures.

Supplementary Material Available: Tables of temperature factor expressions, positional parameters, intramolecular distances and angles, least-squares planes and anisotropic thermal parameters (25 pages). Ordering information is given on any current masthead page.